Design of Bandpass Filter for RF bands Below 6 GHz for 5G Applications

Jamal MESTOUII[1], Mohammed EL GHZAOUI[2] and Abdelhak BENDALI[3]*

[1]ISNT Team, IMAGE Laboratory, Moulay ismail University of Meknes, Morocco
[2]Faculty of Sciences Dhar El Mahraz-Fes, Sidi Mohamed Ben Abdellah University, Fes, Morocco
[3]Laboratory of Electronic Systems, Information Processing, Mechanics and Energy, Morocco

Abstract. The number of frequency bands requiring band-pass filters has improved significantly with the launch of 5G mobile applications. This paper gives an overview of a method for designing a band-pass filter based on low-pass filter parameters. This paper gives an overview of a method for designing a band-pass filter based on low-pass filter parameters. This paper presented a compact microstrip band-pass filter (BPF) covering the spectral bandwidth from 3.4 to 3.8 GHz for 5G wireless communications. The BPF microstrip uses four resonators with 50 Ω transmission line impedances for the input/output terminals. The coupling between the lines is tuned to resonate at the centre frequency with third-order band-pass Butterworth properties. The proposed filter is designed on a Rogers RT/duroid_5870 substrate with a relative dielectric constant ε_r= 2.33. The proposed filter is simulated and optimized using ADS. Simulation results show that the proposed filter works adequately in [3.4 - 3.8 GHz] band and could be considered a good choice for 5G technology.

1 Introduction

Advancing technologies and bandwidth applications have improved mobile data traffic in the radio spectrum. Utilizing spectrum is one of the crucial performance metrics for wireless communication systems. Spectrum efficient techniques used to improve the bandwidth have always been a part of all the generations of wireless communication. Efficient technology is very important to have high spectral, and energy efficiency. Recently, many technologies proved their potential to invoke efficient spectrum utilization. Different approaches have been considered including cognitive radio, machine learning for dynamic spectrum management, spectrum sharing, spectrum harmonization, spectrum identification strategies, etc. [1].

5G technology makes it possible to process much more data at the exact time and ensure the quality of mobile networks, even in very densely populated areas [2-4]. 5G should have a significant impact on society (people and objects). The Need for more data over the wireless network, and the demand for better quality service are among the factors that led to the emergence of the 5G network. One of the largest advantages of wireless systems is their ability to create a global network [5-7].

Spectral efficiency techniques have high importance in 5G networks deployment. Although the COVID-19 pandemic has slowed some 5G deployments, the market continues to multiply as economies recover. Recently, Ericsson released its Mobility Report and raised its forecast for global 5G subscriptions. Ericsson estimates there will be 2.8 billion connections by 2025. The primary technology deployed first in 5G networks is systems Below 6 GHz including low and mid frequencies. The 3.5 GHz band is a popular frequency worldwide, but many more are being rolled out. For the best coverage, a predominant strategy is to use a low-band for rural areas and a mid-band for denser metropolitan areas. [8].

The 5G bands in the mmWave above 24 GHz are attractive to serve fixed connections. For mobile wireless, there are many practical hurdles that will limit the scope and utility for the user [9,10]. Nearly all service providers have planned a rapid deployment of 5G in the sub-6GHz bands, while the use of the mmWave spectrum is mainly driven by chipset companies. For smartphone designers, the introduction of 5G is another assault on battery life and board space. 5th generation (5G) wireless requires RF filters that operate in the bands reserved for emerging applications. Operating at the higher frequencies means power amplifiers are less efficient while antennas and lines have higher losses [11].

2 General operating principle of RF system

Generally, an RF system consists of a transmitter and a receiver. The transmitter's role is to generate the signal to be transmitted and to pass it through the blocks of the transmission chain before sending it to the receiver

* Corresponding author: mestoui@homail.com

through the transmission channel. In addition to helpful information, the transmitter has the role of providing the receiver with information and/or orders that identify it. The receiver to which the call is addressed receives the identifier and the order transmitted by the transmitter, then enters an information exchange scenario with the transmitter.

Figure 1 gives a schematic representation of the general operating principle of an RF system. In this figure also appear the two-radio links: transmitter to receiver called uplink, and receiver to transmitter called downlink.

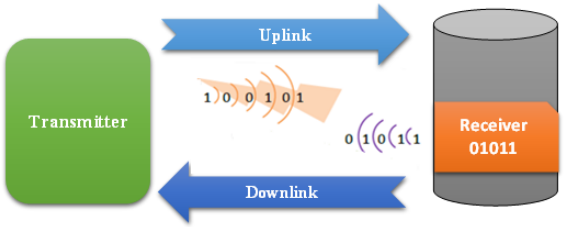

Fig. 1. Operating principle of RF system.

An RF system contains the transmit chain and the receive chain of RF signals. The transmission part shown in Figure 2 is responsible for generating the carrier on which the signal is modulated, for amplifying this signal and transmitting it to the antenna after filtering the useful frequencies. The receive chain shown in Figure 3 processes the signal received from the downlink.

The RF block generally consists of modulation/demodulation components synchronized to a local oscillator.

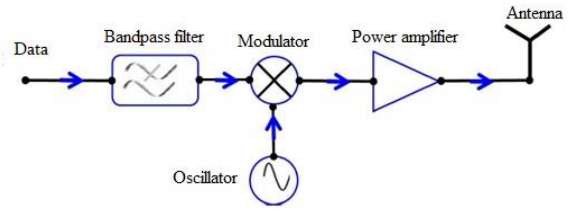

Fig. 2. Components of the transmission chain.

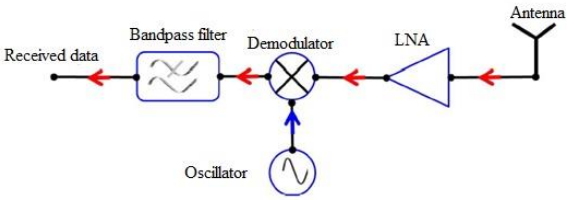

Fig. 3. The components of the reception chain.

Three components play an essential role in radio frequency communication: the filter, the power amplifier and the modulator.

3 Filtering for RF link

The filter is an essential element in current telecommunication systems. It is found at different points of the radio front-end to select the useful signal, on the one hand, and filter the harmonics generated by the non-linear components (amplifiers, oscillators, mixers). The spectral congestion and the proximity of the allocated bands have created constraints in filter performance. To meet specifications, research efforts have focused on the design of a band-pass filter, presenting better responses in bandwidth and amplitude.

The template of a band-pass filter is defined by: ω_0 its centre pulse, ω_1, its low cutoff pulse, and ω_2 its high cutoff pulse.

with

$$\omega_0 = \sqrt{\omega_1 \omega_2} \tag{1}$$

$$\Delta = \frac{\omega_2 - \omega_1}{\omega_0} \tag{2}$$

The frequency transformation from the low-pass plane (ω) to the band-pass plane (ω') is defined by:

$$\omega \rightarrow \frac{1}{\Delta}\left(\frac{\omega_0}{\omega'} - \frac{\omega'}{\omega_0}\right) \tag{3}$$

Obtaining the band-pass filter from the low-pass prototype is done in two steps.

3.1 Design of a band-pass filter by localized elements

First, the series inductors should be replaced by a series LC resonant circuit, with the element values defined as follows [12].

$$C'_k = \frac{\Delta}{\omega_0 L_k} = \frac{\Delta}{\omega_0 g_k} \tag{4}$$

$$L'_k = \frac{L_k}{\Delta \omega_0} = \frac{g_k}{\Delta \omega_0} \tag{5}$$

The second step replaces the capacitors in parallel with a resonant LC circuit in parallel, whose values are as follows [12].

$$C'_k = \frac{C_k}{\Delta \omega_0} = \frac{g_k}{\Delta \omega_0} \tag{6}$$

$$L'_k = \frac{\Delta}{\omega_0 C_k} = \frac{\Delta}{\omega_0 g_k} \tag{7}$$

Localized elements can give two different configurations depending on the starting resonator (series or parallel). The two filter circuits obtained are presented respectively in Figure 4 and Figure 5. The calculation of the values of the series and parallel

resonators (Table 1) is made according to the equations (4), (5), (6) and (7).

with

$g_1 = 1.0315;\ g_2 = 1.1474;\ g_3 = 1.0315;\ g_4 = 1.0$

Table 1. Localized elements values

Series first element	Parallel first element
$L_1^{'} = 82.092\,nH$	$L_1^{'} = 59.521\,pH$
$C_1^{'} = 0.023809\,pF$	$C_1^{'} = 32.837\,pF$
$L_2^{'} = 53.514\ pH$	$L_2^{'} = 82.092\,nH$
$C_2^{'} = 36.523\,nF$	$C_2^{'} = 0.023809\,pF$
$L_2^{'} = 082.092\,nH$	$L_2^{'} = 59.521\,pH$
$C_2^{'} = 0.023809\ pF$	$C_2^{'} = 32.837\,pF$

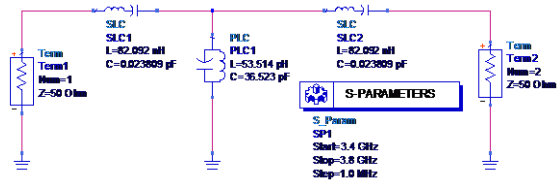

Fig. 4. Localized series elements filter.

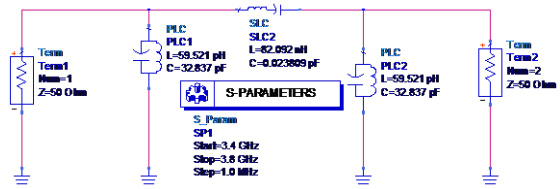

Fig. 5. Localized parallel elements filter.

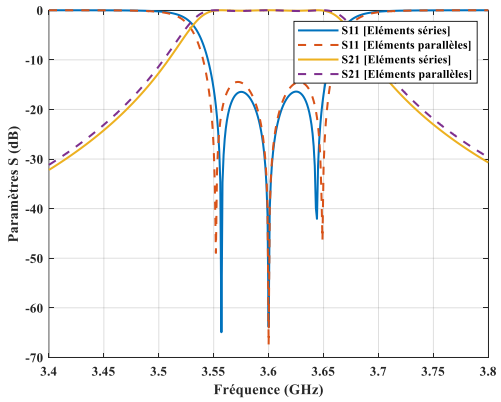

Fig. 6. S-parameters as a function of frequency

Simulation under ADS of the S-parameters of the two circuits in the lower 5G band (3.4-3.8 GHz) gave the results illustrated in Figure 6. The amplitude and phase response of the two band-pass filter circuits are shown in Figure 7 and Figure 8 respectively.

Table 2 summarizes the simulation results of the filter circuit in bandwidth = 100 MHz, phase shift and reflection coefficient S11 at the central frequency 3.6 GHz.

Table. 2. Simulation results

	$S_{11}\ (dB)$	Phase (°)
Series elements	-63.846	-0.029
Parallel elements	-67.494	-0.009

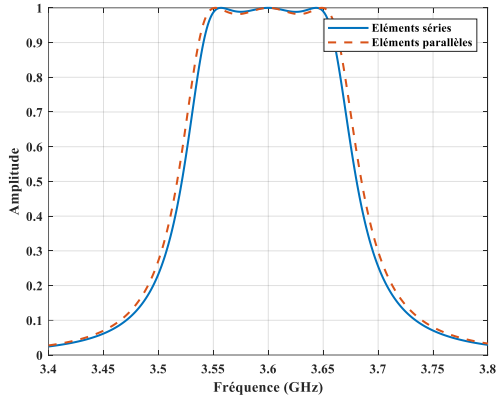

Fig. 7. Amplitude response

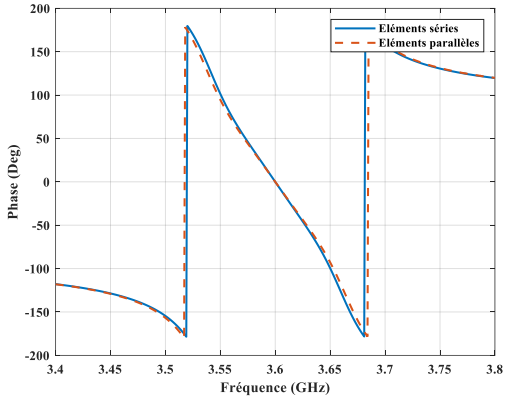

Fig. 8. Phase response

From the simulation results illustrated in Figure 6, Figure 7 and Figure 8, it can be seen that the localized elements are used as basic components for the design of an ideal band-pass filter circuit, in bandwidth. and amplitude response. However, the design with a first series resonator is suitable for having a narrow bandwidth compared to the design with a first parallel resonator.

3.2 Design of the filter with localized elements

The use of ideal lines of the TLIN type (Z, θ) gives results closer to the results obtained with the localized elements. TLINs are not practically available, forcing the switch to the use of microstrip lines, which are widely used in higher frequency scopes. In this section, we present the design of an order three filter with coupled lines to meet the exact specifications mentioned above. There are three types of coupled-line topologies:

quarter-wave coupled-line filters, and half-wave resonators, interdigital resonator filters, and combline filters [13].

Coupled lines are positioned so that adjacent resonators are parallel along half their length. This parallel arrangement gives a relatively large coupling for a given spacing between the resonators; therefore, this filter design is particularly practical for the construction of filters having a narrow bandwidth. The design equations for this type of filters are given [12] :

$$\frac{J_{0,1}}{Y_0}=\sqrt{\frac{\pi.FBW}{2g_0g_1}} \quad (8)$$

$$\frac{J_{j,j+1}}{Y_0}=\frac{\pi.FBW}{2\sqrt{g_j g_{j+1}}} \quad j=1\ à\ n-1 \quad (9)$$

$$\frac{J_{n,n+1}}{Y_0}=\sqrt{\frac{\pi.FBW}{2g_n g_{n+1}}} \quad (10)$$

with FBW is the split bandwidth of the band-pass filter.

The topology of Figure 8 is based on quarter-wave coupled lines, which are put in series giving rise to a half-wave resonator. The order of the filter is equal to N-1 (N: number of coupled lines). The parameters of the parallel-coupled-line filter are calculated using MATLAB code according to equations (8), (9), (10), and equations (11), and (12).

$$(Z_{0e})_{j,j+1}=Z_0\left[1+\frac{J_{j,j+1}}{Y_0}+\left(\frac{J_{j,j+1}}{Y_0}\right)^2\right] \quad (11)$$

$$(Z_{0o})_{j,j+1}=Z_0\left[1-\frac{J_{j,j+1}}{Y_0}+\left(\frac{J_{j,j+1}}{Y_0}\right)^2\right] \quad (12)$$

The values of these parameters are presented in Table3 with j=1 to 3, $\frac{1}{Y_0}=Z_0=50\ \Omega$

and

$g_1=1.0315;\ g_2=1.1474;\ g_3=1.0315;\ g_4=1.0$

Table. 3. Parameters of the parallel coupled line filter

Filter stage number	$\frac{J_{j,j+1}}{Y_0}$	$Z_{0e}\ (\Omega)$	$Z_{0o}\ (\Omega)$
1	0.2057	62.3979	41.8318
2	0.0401	52.0857	48.0751
3	0.0401	52.0857	48.0751
4	0.2057	62.3979	41.8318

To calculate the dimensions of the coupled lines, we used the LineCalc tool from ADS. The substrate used is of the Rogers RT/duroid 5870 type. The filter circuit obtained is shown in Figure 9. After the adaptation and simulation of the S-parameters, we obtained the results shown in Figure 10:

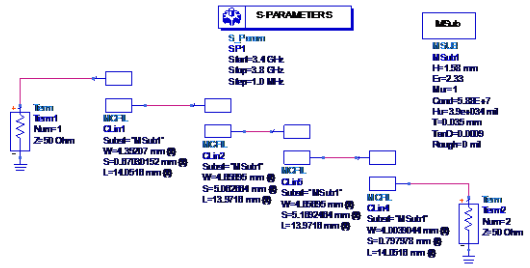

Fig. 9. Line coupled filter on substrate Rogers RT/duroid_5870

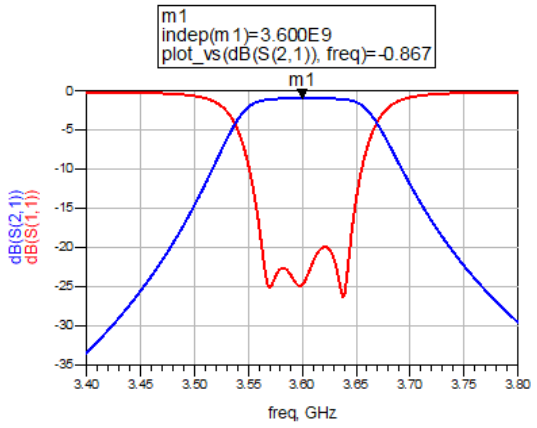

Fig. 10. S(1.1) reflection, and S(2.1) transmission coefficient as a function of frequency

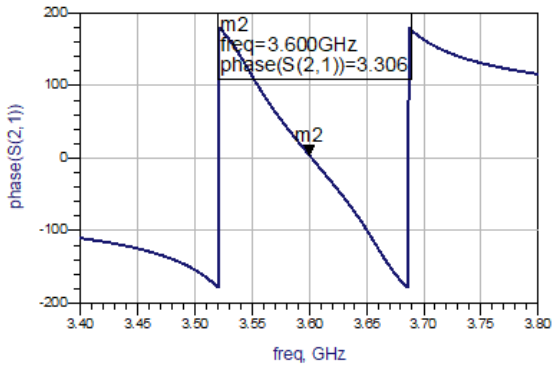

Fig. 11. Phase response of the parallel coupled line filter

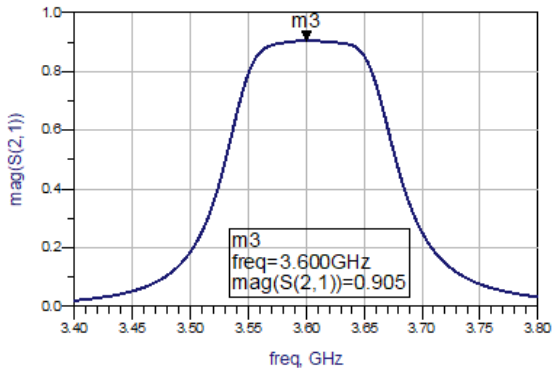

Fig. 12. Amplitude response of the parallel coupled line filter

From these results, it is clear that the design of the coupled line filter, presents a good adaptation with a reflection coefficient S_{11}< -20 dB, and a maximum transmission coefficient S_{21}= -0.867 dB, over a bandwidth of 100 MHz (3.55-3.65 GHz). These values can guarantee an amplitude response of around 90% of the input signal with an acceptable phase shift of 3.306° at the central frequency of 3.6 GHz (Figure 11, and Figure 12). However, this design has a considerable drawback due to the shape of the lines used.

4 Conclusion

This paper presents the design method of a third-order band-pass filter that covers the sub-6 GHz band from 3.4 to 3.8 GHz. The coupling between the lines is set to resonate at the frequency 3.6 GHz. The proposed filter is simulated, and optimized using ADS on a Rogers RT/duroid_5870 type substrate. The suggested filter could be a potential filter for 5G technology at lower band.

References

1. Mihovska, A., Prasad, R. & others. Spectrum Sharing and Dynamic Spectrum Management Techniques in 5G and Beyond Networks: A Survey. *J. Mob. Multimed.* 65–78 (2021).
2. Mestoui, J., Hmamou, A., Foshi, J. & others. BER performance improvement in CE-OFDM-CPM system using equalization techniques over frequency-selective channel. *Procedia Comput. Sci.* **151**, 1016–1021 (2019).
3. Mestoui, J., El Ghzaoui, M., Fattah, M., Hmamou, A. & Foshi, J. Performance analysis of CE-OFDM-CPM Modulation using MIMO system over wireless channels. *J. Ambient Intell. Humaniz. Comput.* 1–9 (2019).
4. El Ghzaoui, M., Hmamou, A., Foshi, J. & Mestoui, J. Compensation of Non-linear Distortion Effects in MIMO-OFDM Systems Using Constant Envelope OFDM for 5G Applications. *J. Circuits, Syst. Comput.* 2050257 (2020).
5. Elaage, S., Ghzaoui, M. El, Hmamou, A., Foshi, J. & Mestoui, J. MB-OOK transceiver design for terahertz wireless communication systems. *Int. J. Syst. Control Commun.* **12**, 309–326 (2021).
6. El Ghzaoui, M., Mestoui, J., Hmamou, A. & Elaage, S. Performance analysis of multiband on--off keying pulse modulation with noncoherent receiver for THz applications. *Microw. Opt. Technol. Lett.* (2021).
7. Aghoutane, B., El Ghzaoui, M. & El Faylali, H. Spatial characterization of propagation channels for terahertz band. *SN Appl. Sci.* **3**, 1–8 (2021).
8. Ericsson, E. Mobility Report: On the Pulse of the Networked Society. *Retrieved from* **31**, (2020).
9. Ghazaoui, Y. *et al.* Millimeter wave antenna with enhanced bandwidth for 5G wireless application. *J. Instrum.* **15**, T01003 (2020).
10. Aghoutane, B. *et al.* Analysis, design and fabrication of a square slot loaded (SSL) millimeter-wave patch antenna array for 5G applications. *J. Circuits, Syst. Comput.* **30**, 2150086 (2021).
11. Aigner, R. *et al.* BAW filters for 5G bands. in *2018 IEEE International Electron Devices Meeting (IEDM)* 14–15 (2018).
12. Hong, J.-S. G. & Lancaster, M. J. *Microstrip filters for RF/microwave applications*. vol. 167 (John Wiley \& Sons, 2004).
13. Mohd Salleh, M. K. Contribution à la synthèse de résonateurs pseudo-elliptiques en anneau: application au filtrage planaire millimétrique. (2008).